

CHARACTERIZATION AND CATALYTIC PERFORMANCE OF POTASSIUM LOADED ON RICE HUSK SILICA AND ZEOLITE NaY FOR TRANSESTERIFICATION OF JATROPHA SEED OIL

Kathrina D. Montalbo and Rizalinda L. de Leon

Department of Chemical Engineering, College of Engineering, University of the Philippines, Quezon City, 1101, Philippines

Onsulang Sophiphun, Saowanee Manadee, Sanchai Prayoonpokarach and Jatuporn Wittayakun*

School of Chemistry, Institute of Science, Suranaree University of Technology, Nakhon Ratchasima 30000, Thailand

Recebido em 22/11/12; aceito em 29/4/13; publicado na web em 17/7/13

Rice husk silica (RHS) and NaY were used as supports for potassium (K) prepared from acetate buffer (B) and acetate (A) solutions. K loading did not destroy the NaY structure, but it caused a decrease in the surface area; the K species resided in micropores and on the external surface. In contrast, K loading resulted in the collapse and a decrease in the surface area of RHS. It was found that 12K/NaY-B was the most active catalyst for the transesterification of Jatropha seed oil. The minimum K content in K/NaY-B that provided complete conversion of the Jatropha seed oil was 11 wt%, and the biodiesel yield was 77.9%.

Keywords: zeolite NaY; potassium; Jatropha seed oil.

INTRODUCTION

Climate change issues, increasing oil prices, and the exhaustion of fossil fuel resources are the main reasons why researchers focus on the development of renewable energy sources and their utilization. One of the renewable energy sources that is being tapped by most countries is biofuel because the transport sector is the largest emitter of pollutants to the atmosphere. Biodiesel is considered as an attractive substitute for petroleum-based diesel fuel because it is an environmentally benign renewable resource that offers the potential for reducing greenhouse gas emissions through a closed CO₂ cycle.¹

Heterogeneous catalysis has become an interesting approach in the production of biodiesel because of the following advantages: heterogeneous catalysts are readily separated from the product and can be recycled, a reduced amount of waste water is produced, and the separation of biodiesel from glycerol is easy.² The use of materials with a high surface area has been investigated as supports for catalysts used in biodiesel production.³ One such material is zeolites, which are microporous crystalline aluminosilicates composed of tetrahedral units of SiO₄ or AlO₄ linked together through shared oxygen atoms. The acid–base properties of zeolites can be modified by changing the Si/Al ratio on the main framework or by changing the type and amount of extra framework cations.⁴

Heterogeneous base catalysis is preferred over acid catalysis because of its faster reaction rate for biodiesel synthesis.⁵ Thus, zeolites with a greater number of basic sites are preferred in the reaction, and the number of basic sites can be increased through a simple impregnation process. Recently, Supamathanon et al.⁶ studied the activity of potassium impregnated on zeolite NaY for the transesterification of Jatropha seed oil to biodiesel. For the catalyst preparation, a CH₃COOK/CH₃COOH buffer solution was used as the potassium precursor. After the impregnated NaY was dried and calcined at 400 °C for 3 h, the zeolite structure was not destroyed. Among the NaY catalysts containing 4, 8, and 12 wt% loaded potassium (notated as 4K/NaY, 8K/NaY, and 12K/NaY, respectively), 12K/NaY provided complete conversion of the Jatropha seed oil and a biodiesel yield of 73.4% under the following conditions: methanol to oil molar ratio of 16:1, 4 w/w% catalyst, reaction time of 3 h, and reaction temperature of 65 °C.

Herein, the results of a comparison of the characteristics and catalytic performance of 12 wt% potassium loaded on different supports (rice husk silica (RHS) and NaY) as catalysts for the transesterification of Jatropha seed oil are reported. Potassium acetate (A) and potassium acetate buffer (B) were used as the active species precursors in order to determine the effect of the potassium precursor on the activity of the catalyst. In addition, the minimum amount of potassium necessary to achieve complete conversion of Jatropha seed oil to biodiesel was determined.

EXPERIMENTAL

Preparation of the catalysts

The extraction of silica from rice husk and the synthesis of zeolite NaY were achieved following previously reported procedures.⁷ The RHS and NaY were then used as catalyst supports. The impregnation of active species on the supports was performed using a wet impregnation method. Buffer solutions containing potassium acetate (CH₃COOK; UNILAB) and glacial acetic acid (CH₃COOH; J.T. Baker) and solutions of CH₃COOK were prepared with different concentrations to produce 9, 10, 11, and 12 wt% potassium on RHS and NaY. For 1.0 g each of RHS and NaY, 2.0 and 1.0 mL of the precursor solution, respectively, was added to produce a slurry. After impregnation, the mixtures were dried at room temperature for 4 h, and then further dried in an oven at 80 °C for 12 h. The dried solids were then ground and calcined at 400 °C for 3 h.

The dispersion of 12 wt% potassium on RHS and NaY was observed visually, and the images of the calcined catalysts were recorded using a personal digital camera. The catalysts were characterized by powder X-ray diffraction (XRD) on a Bruker D5005 X-ray diffractometer with Ni-filtered Cu K α radiation ($\lambda = 1.5406 \text{ \AA}$) generated using 40 kV of electric potential and 40 mA of electric current. The samples were scanned from 5° to 50° with a step of 0.02° and a step time of 0.5 s.

The catalysts were also analyzed using nitrogen adsorption–desorption on Micromeritics ASAP 2010. Prior to analysis, the samples were degassed at 300 °C under vacuum (pressure less than 50 μmmHg). The adsorption–desorption analysis was performed at the boiling temperature of liquid nitrogen (–196 °C), and nitrogen gas

*e-mail: jatuporn@sut.ac.th

was fed and adsorbed onto the sample until the sample was saturated with nitrogen ($P/P_0 = 1$). After the saturation point, the nitrogen was then desorbed by decreasing the pressure. The volume of nitrogen gas adsorbed and desorbed at each specific pressure was recorded.

The exact concentration of potassium in the catalysts was determined via atomic absorption spectroscopy (AAS). The samples were dissolved in an acid solution comprised of 37% HCl (Carlo-Erba), 65% HNO₃ (QR&C), and 4% H₃BO₃ (Merck) and digested in a microwave digester. The digested samples were then diluted to a concentration of 3–10 ppm. The potassium concentration was measured on Perkin Elmer AAnalyst 100 at a wavelength of 766.5 nm using the flame technique.

The active catalysts were characterized using temperature-programmed desorption of CO₂ (CO₂-TPD) on BELCAT-B to determine their basicity. The desorption temperature and amount of desorbed CO₂ are related to the strength and number of basic sites, respectively. The catalyst (0.05 g) was packed into the sample cell and covered with quartz wool. First, the sample was heated at 10 °C/min under a flow of helium (He) from room temperature to 500 °C and then held at this temperature for 60 min. After cooling to 50 °C, CO₂ diluted with inert gas (1% in 99% He) was fed at a rate of 30 mL/min for 30 min. Subsequently, the sample was purged with He for 1 h in order to eliminate any physisorbed species. Thereafter, the temperature was ramped at 10 °C/min to 810 °C. Each CO₂-TPD profile consisted of a plot of the signal intensity as a function of temperature. The basic site densities were then obtained by integrating the areas under the curves.⁸

Transesterification of Jatropha seed oil

The conditions used for the transesterification of Jatropha seed oil were the same as those reported in the study by Supamathanon et al.⁶ The catalyst was initially dried at 100 °C for 12 h and then ground. Precisely 0.2 g of the ground catalyst was mixed with 5.0 g of Jatropha seed oil and 2.9 g of methanol in a 50-mL round bottom flask. The flask was then heated in a water bath at 65 °C, and the mixture was stirred for 3 h. After the reaction, the mixture was cooled to room temperature and the catalyst was separated by centrifugation. The product mixture was decanted to a separatory funnel, which was closed and left overnight to allow complete phase separation. The biodiesel (upper layer) was then collected, and the remaining methanol was removed using a rotary evaporator (Büchi Rotavapor R-114).

The Jatropha seed oil conversion to biodiesel was estimated by thin layer chromatography (TLC). The biodiesel obtained from the reaction was spotted on a TLC plate (Silica Gel 60 F254; Merck, Darmstadt, Germany). Thereafter, the plate was developed using a carrier solvent mixture consisting of petroleum ether (8.5 mL; J.T. Baker), diethyl ether (1.5 mL; AR grade, C₄H₁₀O, QR&C), and glacial acetic acid (0.1 mL). The plate was then dried and exposed to iodine vapor (UNICROM) to make the spots visible. The images of the TLC plates after exposure to iodine vapor were recorded using a digital camera.

The biodiesel yield, which was considered to be the sum of the methyl esters in the biodiesel product, was determined using a gas chromatograph (Hewlett Packard HP 6890 Plus) equipped with a flame ionization detector (FID) and 30-m HP-INNOWAX polyethylene glycol capillary column (0.32 mm internal diameter and 0.15 mm film thickness). The detector temperature was 250 °C, and the injection volume and temperature were 1 µL and 220 °C, respectively. The initial column temperature was held at 140 °C for 3 min, then ramped to 240 °C at a rate of 10 °C/min, and held for another 10 min. The biodiesel yield was calculated using the following equation:⁶

$$\% \text{ yield} = \frac{(C_{\text{ester}} \times n)}{\rho_{\text{oil}}} \times 100$$

where C_{ester} is the concentration of methyl ester in g/mL, n is the diluted multiple of the methyl esters, which is the total volume of n -hexane and the internal standard solution divided by the volume of the methyl ester sample, and ρ_{oil} is the density of the Jatropha seed oil, which was 0.91 g/mL.

Prior to yield determination, the mass concentration of each methyl ester was obtained from a separate calibration curve constructed using methyl ester standards that were obtained from Sigma, including those of palmitic (C₁₇H₃₄O₂, P5177), palmitoleic (C₁₇H₃₂O₂, P9667), heptadecanoic (C₁₈H₃₆O₂, H4515), stearic (C₁₉H₃₆O₂, S5376), oleic (C₁₉H₃₆O₂, O4754), linoleic (C₁₉H₃₄O₂, L1876), linolenic (C₁₉H₃₂O₂, L2626), and arachidic (C₂₁H₄₂O₂, A3881) acids. The methyl ester of nonadecanoic acid (C₂₀H₄₀O₂, N5377) was used as an internal standard.

RESULTS AND DISCUSSION

Characteristics of RHS impregnated with CH₃COOK/CH₃COOH and CH₃COOK

The images of extracted RHS and RHS loaded with 12 wt% potassium using CH₃COOK/CH₃COOH (12K/RHS-B) and aqueous CH₃COOK (12K/RHS-A) are shown in Figure 1S (a–c) in the Supplementary Material. After the rice husk was leached using 3 M HCl and calcined at 550 °C, a white powder containing SiO₂ was obtained (Figure 1S (a)). After calcination, 12K/RHS-B appeared as a white powder with random spots of grey powder (Figure 1S (b)), which could be carbonaceous compounds generated from the thermal decomposition of acetate and acetic acid that were encapsulated in the silica. This encapsulation could occur if the pores of silica collapsed during the heat treatment. It has been reported that the presence of potassium may cause the melting of the silica surface and accelerate the crystallization of amorphous silica to cristobalite.⁸ Such a collapse would also result in a lower surface area. In the case of calcined 12K/RHS-A, there was a greater quantity of the dark powder (Figure 1S (c)). It is possible that the acetate solution induced a faster collapse of the silica pores and resulted in more carbon encapsulation. If the structure collapsed, the potassium oxide generated after calcination could also be trapped within the silica, and thus, it may not be accessible for catalytic reactions. The changes in phase, surface area, and number of accessible basic sites were confirmed by XRD, N₂ adsorption–desorption, and CO₂-TPD analysis, respectively.

The XRD patterns of RHS (Figure 1) contained only a broad peak that is characteristic of amorphous phase silica. In the patterns of 12K/RHS-B and 12K/RHS-A, the broad band decreased, indicating that the solid became denser. The collapse of the RHS porous structure likely occurred and led to the decrease in the intensities of the XRD patterns.⁹ Calcination at 400 °C was sufficient to decompose potassium acetate to potassium oxide because peaks for potassium acetate

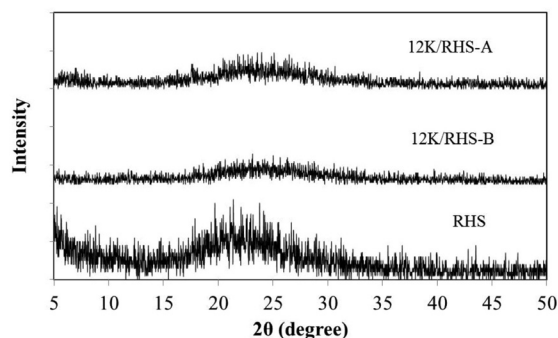


Figure 1. XRD patterns of RHS, 12K/RHS-B, and 12K/RHS-A

at $2\theta = 8.26^\circ$ and 6.49° ¹⁰ were not observed in the XRD patterns. The peaks for potassium oxide at $2\theta = 31^\circ$ and 39° ¹¹ were also not observed, indicating that the potassium was well dispersed on the support.

The N_2 adsorption–desorption isotherm for RHS (Figure 2) was a type IV according to the IUPAC classification. The adsorption increased rapidly at the beginning because of adsorption of N_2 both into micropores and on the external surface. The adsorption then increased gradually over the entire pressure range, indicating multilayer adsorption. A hysteresis loop was observed beginning at a relative pressure of 0.45, which corresponded to the capillary condensation of the adsorbate in nonuniform mesopores.^{12,13} On the other hand, the isotherms for 12K/RHS-B and 12K/RHS-A showed much lower adsorptions than the parent RHS, indicating that both catalysts had a very low surface area. The impregnation of RHS using both precursor solutions and the following heat treatment caused the collapse of both the micropores and mesopores of the RHS. Table 1 lists the surface areas of the catalysts determined using the Brunauer–Emmett–Teller (BET) method, micropore area, and micropore volume. The surface area of RHS was 301 m^2/g ; however, after loading of potassium with either CH_3COOK/CH_3COOH or CH_3COOK , the surface area drastically dropped. The significant decrease in the surface area is due to occlusion of the metal oxide on the surface of the support and the collapse of the structure resulting from “dissolution” of the surface by the alkali solutions during impregnation and fusion of SiO_2 particles.¹⁴

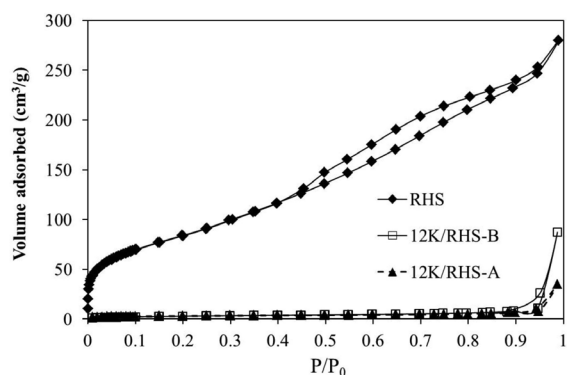


Figure 2. Nitrogen adsorption–desorption isotherms for RHS, 12K/RHS-B, and 12K/RHS-A

Table 1. Textural properties of RHS and NaY before and after impregnation with CH_3COOK/CH_3COOH or aqueous CH_3COOK and calcination at 400 °C for 3 h

Sample	BET surface area (m^2/g)	Micropore area (m^2/g)	Micropore volume (cm^3/g)	Average pore size (\AA)
RHS	301	35	0.02	58
12K/RHS-A	10	2	0.00	212
12K/RHS-B	11	3	0.00	497
NaY	927	855	0.40	22
12KNaY-A	232	223	0.11	31
12KNaY-B	299	265	0.13	27
11KNaY-B	329	295	0.14	29
10KNaY-B	390	351	0.17	27
9KNaY-B	424	384	0.18	28

Characteristics of NaY impregnated with CH_3COOK/CH_3COOH and CH_3COOK

The image of calcined 12K/NaY-B (Figure 2S (a) in the Supplementary Material) showed a homogeneous white powder,

suggesting that the hydrocarbon compounds from the potassium precursors were completely removed from 12K/NaY-B without leaving any carbon residue. In contrast, the photo of calcined 12K/NaY-A (Figure 2S (b) in the Supplementary Material) contains random grey spots, which could be carbon residue encapsulated in the silicate structure after the collapse of the zeolite. The characteristics of 12K/NaY-B and 12K/NaY-A were further studied via XRD, nitrogen adsorption–desorption, and CO_2 -TPD analysis to determine any changes in the zeolite phase, textural properties, and basicity, respectively.

Figure 3 shows the XRD patterns of 12K/NaY-B and 12K/NaY-A compared with that of the parent zeolite. After impregnation using both solutions and heat treatment, the characteristic peaks of NaY were still observed in both 12K/NaY-B and 12K/NaY-A but with a significant decrease in the peak intensities. These results indicated that the zeolite structure was preserved upon impregnation and calcinations; however, some collapse of the structure may have occurred. In addition, the peak intensities in the XRD pattern of 12K/NaY-B were higher than those of 12K/NaY-A, indicating that the use of potassium acetate buffer preserved the NaY structure better than the use of potassium acetate alone. The XRD analysis of the zeolite impregnated with water and then calcined was also performed. The characteristic peaks of zeolite NaY were still observed in this material with no significant difference in the intensities compared with those observed for the untreated zeolite, suggesting that the partial damage of zeolite after impregnation is not mainly due to the thermal treatment during the calcination process. Therefore, the decrease in the intensity of the NaY peaks in the XRD pattern after potassium loading are mainly due to the hydrolysis of Si–O–Al bonds by the alkali metal during the thermal treatment of the zeolite.¹⁵ Hydrolysis may have occurred to a greater extent when potassium acetate was used because it is more basic than the acetate buffer solution. The pH of the acetate buffer and acetate solutions were 4.5 and 8.5, respectively. Finally, as with the RHS catalysts, calcination at 400 °C was sufficient to decompose potassium acetate to potassium oxide because the peaks for potassium acetate were not observed. In addition, the phases of potassium oxide were not observed, indicating good dispersion of potassium oxide on the support.

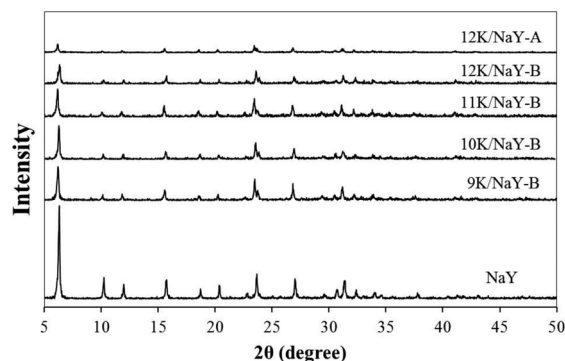


Figure 3. XRD patterns of the NaY, K/NaY-B catalysts with K loadings of 9, 10, 11, and 12 wt%, and 12K/NaY-A

Note that 12K/NaY-B was also calcined at higher temperatures (500 °C and 600 °C), and the XRD patterns are shown in Figure 3S in the Supplementary Material. Calcination at 600 °C produced the new species α - K_2O and $NaAlSiO_4$ (peaks at $2\theta = 28.9^\circ$ ¹¹ and 34.7° ¹⁰ respectively). This result indicated that amorphization and collapse of the zeolite structure occurred during calcination at higher temperatures. Because of the collapse of the structure, the active species may have been trapped in the amorphous phase, thus hindering reactivity.¹⁶ Therefore, these catalysts were not tested in the transesterification reaction.

Furthermore, the NaY catalysts were analyzed using nitrogen adsorption–desorption (Figure 4). Both 12K/NaY-B and 12K/NaY-A showed type I isotherm characteristics of microporous substances; the adsorption of nitrogen increased abruptly at a low relative pressure (P/P_0). A lower amount of adsorbed nitrogen was measured for 12K/NaY-B and 12K/NaY-A compared with that for the parent zeolite, indicating that the micropores were occupied. However, the adsorbed volume on 12K/NaY-B was greater than that on 12K/NaY-A. The values for the surface areas and micropore volumes are summarized in Table 1.

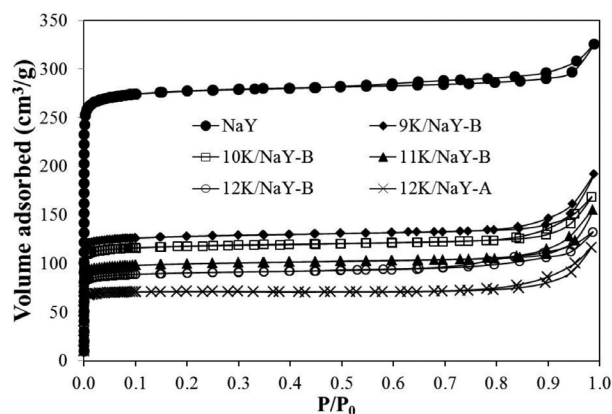


Figure 4. Nitrogen adsorption–desorption isotherms for NaY, K/NaY-B catalysts with K loadings of 9, 10, 11, and 12 wt%, and 12K/NaY-A

The relatively lower values for the surface area, micropore area, and micropore volume obtained for NaY loaded with K metal indicated that the metal particles resided on the external surface and in the pores of the zeolite. Moreover, the lower values obtained for 12K/NaY-A may be because of amorphization or collapse of the structure. The use of acetate solution with pH = 8.5, which is higher than that of the buffer solution (pH = 4.5), may cause greater hydrolysis of the Si–O–Al bonds in the zeolite framework.¹⁶ Therefore, it can be concluded that the use of a buffer solution may preserve the zeolite structure, and thus lead to improvement in the catalytic activity.

The CO₂-TPD profiles for 12K/RHS-B, 12K/RHS-A, 12K/NaY-B, and 12K/NaY-A are shown in Figure 5. The desorbed amounts from the RHS-supported catalysts were low, suggesting limited accessibility to the basic sites. Thus, these catalysts were not expected to be very active for the transesterification reaction. In contrast, the desorbed amounts from the NaY-supported catalysts were significantly higher, suggesting high accessibility to the basic sites. The major desorption occurred between 550 °C and 800 °C, which corresponds

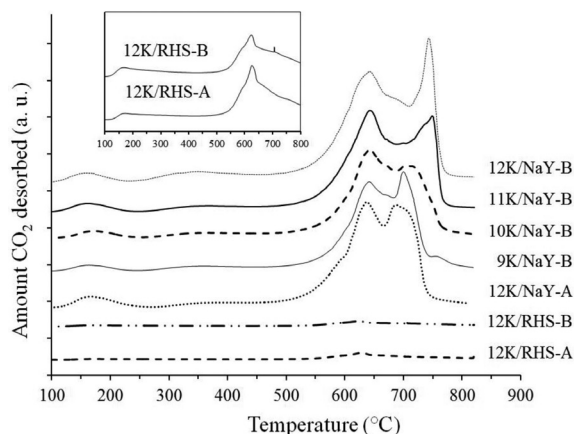


Figure 5. CO₂-TPD profiles of the 12K/RHS-B, 12K/RHS-A, 12K/NaY-A, and K/NaY-B catalysts with K loadings of 9, 10, 11, and 12 wt%

to a strong basicity. Ramos et al. reported that strong basic sites on zeolite NaX (similar framework type to NaY) loaded with Na via impregnation were centered around 700 °C in the CO₂-TPD profile and corresponded to clusters of oxides in the zeolite cavity.¹⁷ In addition, the peak area from the CO₂-TPD profile for 12K/NaY-B was larger than that for 12K/NaY-A, suggesting that the catalyst prepared from the acetate buffer solution had a higher basicity.

Next, the K/NaY catalysts with different amounts of potassium (i.e., 9, 10, 11, and 12 wt% K) were also prepared using the acetate buffer solution. The catalysts were characterized by XRD, N₂ adsorption–desorption, and CO₂-TPD analysis. The XRD patterns (Figure 3) showed that as the amount of metal loading increased, the intensity of the peaks decreased, corresponding to a decrease in the crystallinity due to agglomeration of the oxide species in the cavity of the zeolite.¹⁸ The presence of the characteristic peaks of the parent zeolite after metal loading indicated the preservation of the zeolite structure. The absence of K₂O peaks indicated a good dispersion of the metal oxide throughout the zeolite surface.^{6,12}

In the nitrogen adsorption–desorption isotherms of the catalysts with different potassium loading (Figure 4), it was observed that the surface area decreased with an increase in potassium loading with a linear relationship ($R^2 = 0.98$). In addition, the external surface area, micropore area, and micropore volume of the catalysts were all lower than those of the parent zeolite NaY (Table 1) and tended to decrease with an increase in potassium loading. These results indicated that the active species occluded in the micropores of the zeolite and resided on the external surface.

The CO₂-TPD profiles of the K/NaY-B catalysts with K loadings of 9, 10, 11, and 12 wt% are shown in Figure 5. The desorption of CO₂ from all catalysts occurred over a similar temperature range that indicated strong basicity. On the basis of the values obtained for integration of the total peak areas, it was found that the basicity increased with potassium loading: 5.93, 6.15, 7.24, and 8.25 mmol CO₂/g-catalyst for K loadings of 9, 10, 11, and 12 wt %, respectively.

Catalytic performance for transesterification of crude *Jatropha* seed oil to biodiesel

The prepared catalysts on RHS and NaY supports were used in the transesterification of *Jatropha* seed oil to produce biodiesel. Fatty acid methyl ester standards, crude *Jatropha* seed oil, and the products were spotted on a TLC plate to qualitatively analyze the reaction. In addition, both supports (RHS and NaY) were tested for transesterification using a similar procedure. The results of the TLC analyses (not shown) indicated that neither support was active for transesterification.

Figure 6 (a–d) presents the TLC plates for the transesterification products using catalysts with 12 wt% K loaded on RHS and NaY. A low conversion of the transesterification product was observed using the catalysts with RHS as the support (Figure 6 (a,b)). These catalysts have few active sites for transesterification because of their low surface area and potassium may also be dislocated in the amorphous surface of the silica, making it unavailable to the reactants.¹⁵ In addition, the results for the conversion of *Jatropha* seed oil to biodiesel using 12K/RHS-B and 12K/RHS-A were not significantly different. The instability of the structure and low surface area made RHS undesirable as a catalyst support. On the other hand, the NaY-supported catalysts showed better conversion than the RHS-supported catalysts (Figure 6 (c,d)). Supamathanon et al.⁶ reported that 12 wt% K loaded on NaY using a buffer solution showed complete conversion of *Jatropha* seed oil to biodiesel. This result is also observed with 12K/NaY-B (Figure 6 (c)). In contrast, 12K/NaY-A, which was prepared by impregnation of 12 wt% K on NaY using aqueous CH₃COOK, showed incomplete conversion of *Jatropha* seed oil to

biodiesel (Figure 6 (c)). These results are in good agreement with the previous characterization results for this catalyst. The catalyst prepared without using the buffer solution, as previously discussed, had a lower surface area and lower crystallinity compared with the catalyst prepared using the $\text{CH}_3\text{COOK}/\text{CH}_3\text{COOH}$ mixture, and thus, it exhibited lower reactivity.

After testing the catalysts with 12 wt% K, it was determined that 12K/NaY-B was the most effective catalyst. Supamathanon et al.⁶ compared the reactivity of catalysts with different amounts of potassium loading, i.e., 4, 8, and 12 wt% K loaded on NaY using a $\text{CH}_3\text{COOK}/\text{CH}_3\text{COOH}$ mixture as the active species precursor, with 12K/NaY being the most effective catalyst. In the current study, the activity of catalysts with potassium loadings lower than 12 wt%, i.e., 9, 10, and 11 wt% K loaded on NaY, was also tested. The products of the transesterification reactions spotted on the TLC plates are shown in Figure 6 (e–h).

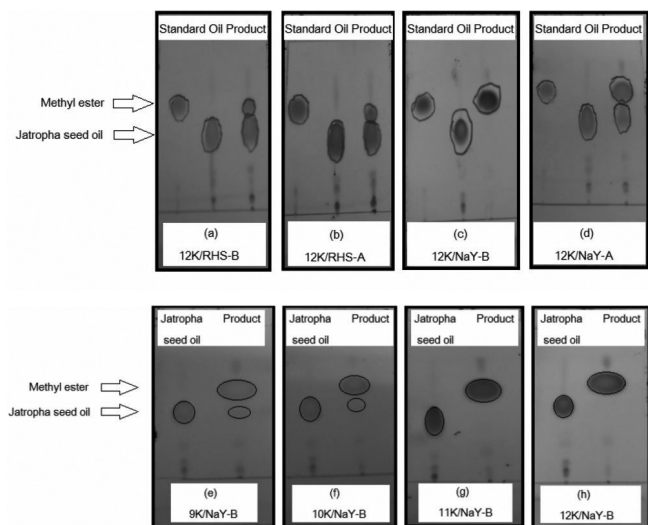


Figure 6. TLC plates of the transesterification products using (a) 12K/RHS-B, (b) 12K/RHS-A, (c) 12K/NaY-B, (d) 12K/NaY-A, (e) 9K/NaY-B, (f) 10K/NaY-B, (g) 11K/NaY-B, and (h) 12K/NaY-B

The TLC plates showed increasing conversion when potassium loading was increased and complete conversion was observed for 11K/NaY-B and 12K/NaY-B. This result indicated that the minimum amount of metal loading on NaY that provided complete conversion of Jatropha seed oil to biodiesel was 11 wt%. Next, to confirm the actual amount of potassium in the catalysts with different potassium loadings, the potassium concentration was determined by AAS. The actual weight of K in 9K/NaY-B, 10K/NaY-B, 11K/NaY-B, and 12K/NaY-B was confirmed to be 7.91, 9.35, 10.32, and 11.04 wt%, respectively. Hence, the minimum weight of K loaded on NaY that provided complete conversion of the Jatropha seed oil was 10.3 wt%. The loadings as determined by AAS were lower than the calculated values because the catalysts were prepared via wet impregnation with a slurry of NaY in the precursor solution. A part of the solution adhered to the container, resulting in lower K loadings on the NaY.

The products of the transesterification reactions obtained using the catalysts that gave complete conversion as observed by TLC analysis were further analyzed using GC-FID. The yields of biodiesel obtained with 11K/NaY-B and 12K/NaY-B were 77.9 and 77.2%, respectively.

CONCLUSIONS

This study utilized RHS and zeolite NaY as supports for potassium, which was supplied in the form of either acetate buffer (B) or

acetate (A) solutions. The zeolite NaY catalysts had higher surface areas and greater stability upon impregnation and calcination than the RHS catalysts, which collapsed after catalyst preparation. Hence, the NaY-supported catalysts were more active than the RHS-supported ones. In addition, the surface area of 12K/NaY-A was lower than that of bare NaY and 12K/NaY-B, indicating that the zeolite structure of 12K/NaY-A experienced a greater level of collapse, thus resulting in lower basicity and catalytic activity for the transesterification reaction.

Furthermore, the surface area of the NaY-supported catalysts decreased and the basicity increased as K loading increased. The catalyst with the least potassium loading that gave complete conversion of Jatropha seed oil to biodiesel was found to be 11K/NaY-B. The actual amount of potassium in this catalyst was determined by AAS to be 10.32 wt%, and the biodiesel yield with this catalyst was 77.9 %.

ACKNOWLEDGMENT

This research was supported by the Suranaree University of Technology, Thailand.

SUPPLEMENTARY MATERIAL

Figures 1S–3S are available at <http://quimicanova.sbg.org.br>, in a PDF file, with free access.

REFERENCES

- Narasimharao, K.; Lee, A.; Wilson, K.; *J. Biobased Mater. Bio.* **2007**, *1*, 19.
- Singh Chouhan, A.; Sarma, A.; *Renew. Sust. Energ. Rev.* **2011**, *15*, 4378.
- Semwal, S.; Arora, A. K.; Badoni, R. P.; Tuli, D. K.; *Bioresour. Technol.* **2011**, *102*, 2151; Endalew, A.; Kiros, Y.; Zanzi, R.; *Energy* **2011**, *36*, 2693.
- Schen, U.; Hunger, M.; Weitkamp, J.; *Magn. Reson. Chem.* **1999**, *37*, S75; Suppes, G.; Dasari, M.; Doscocil, E.; Mankidy, P.; Goff, M.; *Appl. Catal. A Gen.* **2004**, *257*, 213.; Wang, Y.-Y.; D ang, T. H.; Chen, B.-H.; Lee, D.-J.; *Ind. Eng. Chem. Res.* **2012**, *30*, 9959.
- Lee, D.-W.; Park, Y.-M.; Lee, K.-Y.; *Catal. Surv. Asia* **2009**, *13*, 63.
- Supamathanon, N.; Wittayakun, J.; Prayoonpokarach, S.; *J. Ind. Eng. Chem.* **2011**, *17*, 182.
- Wittayakun, J.; Khemthong, P.; Prayoonpokarach, S.; *Korean J. Chem. Eng.* **2008**, *25*, 861.
- Krishnarao, R.V.; Subrahmanyam, J.; Jagadish Kumar, T.; *J. Eur. Ceram. Soc.* **2001**, *21*, 99.
- Zhao, X. S.; Lu, G. Q. Hu, X.; *Microporous Mesoporous Mater.* **2000**, *41*, 37.
- JCPDS; *Powder Diffraction File, Alphabetical Indexes, Inorganic Phases*, Sets 1-48, USA, 1998.
- Noiroj, K.; Intarapong, P.; Luengnaruemitchai, A.; Jai-In, S.; *Renewable Energy* **2009**, *34*, 1145.
- Farrauto, R. J.; Hobson, M. C.; In *Encyclopedia of Physical Science and Technology*; Meyers, R. A., ed.; Academic Press, 1992, p. 736.
- Jentys, A.; Lercher, J. A.; *Stud. Surf. Sci. Catal.* **2001**, *137*, 345.
- Bal, R.; Tope, B. B.; Das, T. K.; Hegde, S. G.; Sivasanker, S.; *J. Catal.* **2001**, *204*, 358.
- Simon, A.; K hler, J.; Keller, P.; Weitkamp, J.; Buchholz, A.; Hunger, M.; *Microporous Mesoporous Mater.* **2004**, *68*, 143.
- Man, W. K.; Ramli, Z.; Nur, H.; *Jurnal Teknologi*, **2005**, *42(C)*, 43.
- Ramos, M. J.; Casas, A.; Rodr guez, L.; Romero, R.; P rez, A.; *Appl. Catal. A Gen.* **2008**, *346*, 79.
- Romero, M. D.; Ovejero, G.; Rodr guez, A.; Gomez, J. M.; *Microporous Mesoporous Mater.* **2005**, *81*, 313.